



# COMP 6771 – Image Processing Project - Fall 2023

Topic: Blood Vessel Filtering and Extraction

Ronak Patel, Student ID: 40221814

# Contents

1	Part 1 . . . . .	2
1.1	Retinal vessel extraction by matched filter with first-order derivative of Gaussian . . . . .	2
1.2	Retinal Blood Vessel Extraction from Fundus Images Using Enhancement Filtering and Clustering . . . . .	3
2	Re-implementation of the Main Algorithm — Part 2 . . . . .	4
2.1	Our Re-Implemented Algorithm . . . . .	4
2.2	Implemented Algorithm Validation . . . . .	5
	References . . . . .	11

## 1 Part 1

### 1.1 Retinal vessel extraction by matched filter with first-order derivative of Gaussian

Zhang et al. (2010)[4] introduced an improved approach for extracting retinal blood vessels from retinal images using a matched filter with the first-order derivative of Gaussian. The importance of this research was to accurately depict the blood vessels for various imaging applications, particularly in diabetic retinopathy.

The paper proposed an idea of combining the approach of matched filter with first-order derivative of Gaussian (MF-FDOG) for enhancing sensitivity and specificity of vessel detection with little to no false positives.

The main advantage of classical matched filter is simplicity and effectiveness. It utilizes prior knowledge of cross section of a vessel is gaussian shape to match the vessel for the detection. However, the main issue is that it also detects non-edges like bright blobs in the images.

To address the limitations and exploit further information on vessels, Zhang et al[4] used FDOG with matched filter. The reason for this is that the true vessel will have a strong response to MF, while local mean of response would be almost zero for FDOG. On the other hand, step edges will behave similarly to MF but its response to FDOG will be high, and this allows them to remove those edges. Moreover, only utilizing FDOG is challenging because of fast changing magnitude around Gaussian peaks, which hinders the differentiation of true edges to step edges.

MF-FDOG method contains several steps. Initially, MF is applied to the retinal image and response  $H$  is generated. After FDOG is applied to get response  $D$ . to get the edge map we can apply threshold  $T$  based on FDOG response to detect step edges and extract only true edges. This simple yet effective approach discards the drawbacks of MF.

MF-FDOG approach proves to be efficient. The experiment data, when compared to another novel methods looks promising. This method has some of the highest accuracy and low false positive rate when using STARE database. However, with different database DRIVE, the end results are average compared to other given methods but the trend of being far superior to MF method is still consistent. One of the reasons for inferior results while using DRIVE database is that it uses predominantly normal image compared to pathological retinal images in STARE database. In conclusion, the given method in the paper aims to improve the classic MF approach to a far greater extent while being less complex and efficient.

The authors have done magnificent work and presented competitive and simple methods for vessel detection. However, the paper could give us more detailed analysis on several factors with various prestigious approaches. Also, more information on limitations of MF-FDOG method would be helpful for adaptability and testing of the algorithm under certain scenarios.

## 1.2 Retinal Blood Vessel Extraction from Fundus Images Using Enhancement Filtering and Clustering

The paper "Retinal Blood Vessel Extraction from Fundus Images Using Enhancement Filtering and Clustering" [2] Dash et al. is also concerned about the detection of retinal blood vessels from fundus images. The paper provides an unsupervised approach to extract the vessels using a method with multiple stages of processing the image for certain outcome. The inspiration for using an unsupervised approach is eliminating the need for training and making the process more accessible for implementation.

The strength of this paper lies in its detailed approach to extracting the vessels. This process is divided into three parts, pre-processing, segmentation and post-processing. It starts by enhancing vessels by Contrast Limited Adaptive Histogram Equalization (CLAHE), after feature extracting using Gabor filter, which is followed by Hessian-based enhancement filtering. The use of K-mean clustering is essential to differentiate the vessels. Finally, morphological cleaning is applied to get refined results.

Comparing this process to Zhang et al. (2010)'s MF-FDOG method, Dash et al.'s [2] method is more focusing on unsupervised learning while counterpart is more focusing on enhancing vessel detection accuracy through filtering and using derivation. Both methods aim to achieve singular outcome. However, the complexity of Dash et al.[2]. is definitely higher than Zhang et al[4]. Due to involving multiple stages in processing, which is more sophisticated and resulting in better outcome. On the other hand, the simplicity of the MF-FDOG algorithm is desirable considering its above average outcome.

This paper excels at providing the experiment results. Not only does it outshine Zhang et al[4] in many aspects, but it does compare its outcome with many other industry leading methods (supervised and unsupervised) and across various criteria of the algorithm. It takes various aspects into account like Sensitivity (Se), Specificity (Sp), Accuracy (ACC), False Discovery Rate (FDR) and more. They also have conducted results on DRIVE and CHASE\_DB1, recording different parameters. It outperforms many existing methods in DRIVE with ACC of 0.952 and in CHASE\_DB1 with ACC of 0.951. These results are more accurate than MF-FDOG's average ACC of 0.938 in DRIVE database. Dash et al.[2] Also presents metrics for correctly detecting thin vessels, which are harder to find, and performs well with ACC of 0.953 and 0.944 for DRIVE and CHASE\_DB1, respectively.

So, in the end, both algorithms use unsupervised learning approach but Dash et al.'s[2] method to applying series of processing stages might be more complex than straightforward way of MF-FDOG's approach. Furthermore, trade off between computation/complexity and accuracy seems to justify both presented algorithms.

## 2 Re-implementation of the Main Algorithm — Part 2

### 2.1 Our Re-Implemented Algorithm

Algorithm Notations:

Symbol	Description
$FDOG$	First-order derivative of Gaussian
$MF$	Matched Filter
$L$	Length of the neighborhood along the Y-axis for noise smoothing
$s$	Scale of the filter
$W$	$w \times w$ filter with elements all equal to $1/w^2$
$c$	Constant (between 2 and 3 based on empirical experience)
$H$	Response map from $MF$
$D$	Response map from $FDOG$
$D_m$	Local mean image of $D$
$D_m^{\text{complement}}$	Local mean image of $D$ complement
$\mu H$	Mean value of response image $H$
$T_c$	Reference threshold calculated as $c \cdot \mu H$
$T$	Image threshold value
$M_h$	Binary thresholded image (1 or 0) based on threshold $T$
$H(x, y)$	Pixel value at position $(x, y)$ of Image $H$
$T(x, y)$	Pixel value at position $(x, y)$ of Image $T$

Table 1: Symbol Descriptions

**Pre Preprocessing Steps:**

1. Convert the image to grayscale.
2. Apply average smoothing to the image for noise reduction.

**Algorithm Steps:**

1. **Compute Response Images  $h$  and  $d$  using  $MF$  and  $FDOG$** 
  - Compute  $h$  and  $d$  for  $MF[1]$  and  $FDOG[4]$ , respectively.
2. **Obtain Max Responses to Form  $H$  and  $D$** 
  - Get the maximum responses from the lists of  $MF$  and  $FDOG$  responses at different angles to create  $H$  and  $D$  images.
3. **Calculate Local Mean Image  $D_m$** 
  - Compute the local mean image  $D_m$ .

#### 4. Determine Threshold Value $T$

- (a) Specify the average filter  $W$  with each element's value as  $1/w^2$ .
- (b) Apply  $W$  to  $D$  to obtain  $D_m$ .
- (c) Normalize  $D$  to the range  $[0, 1]$  to create  $D_m^{\text{complement}}$ .
- (d) Calculate the mean value  $\mu H$  of the response image  $H$ .
- (e) Compute the reference threshold  $T_c = c \cdot \mu H$ .
- (f) Calculate the final threshold  $T = (1 + D_m^{\text{complement}}) \cdot T_c$ .

#### 5. Apply Threshold $T$ to $H$

- Threshold each pixel in  $H$  by comparing  $H(x, y)$  to  $T(x, y)$ . If  $H(x, y) \geq T(x, y)$ , set  $M_h(x, y) = 1$ , otherwise, set  $M_h(x, y) = 0$ .

$M_h$  is the final binary thresholded image.

## 2.2 Implemented Algorithm Validation

### Optimal Results

We used the following image as the base input for running the algorithm. On the left side of Figure 1 is the original RGB image, and on the right side is the grayscale version.

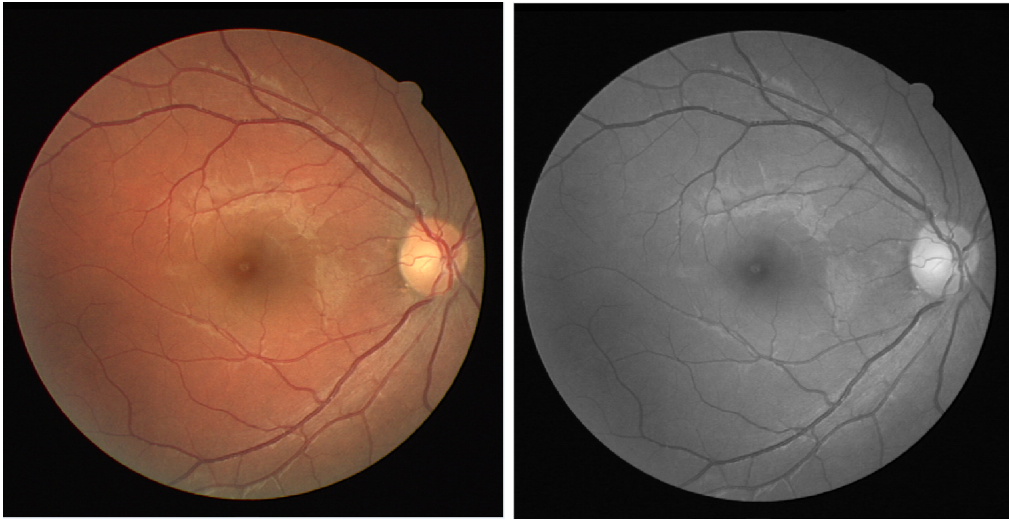


Figure 1: Original RGB Image (Left) and Grayscale Image (Right)

We executed the algorithm with the best-performing parameters as outlined in the paper:  $s = 1.5$ ,  $L = 9$  for detecting wide vessels, and  $s = 1$  and  $L = 5$  for detecting thin vessels, using a  $31 \times 31$  filter with  $c = 2.3$ . The results are shown below Figure 2,

where the left image displays the detection of thin vessels, and the right image shows the detection of thick vessels[3]. The algorithm demonstrates excellent performance.

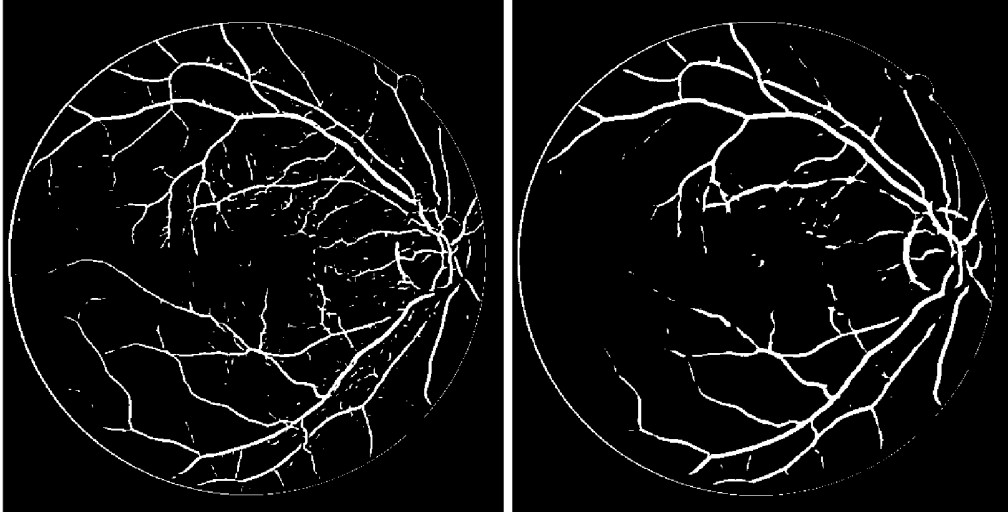


Figure 2: Thin Vessels Detection (Left) and Thick Vessels Detection (Right)

To detect both types of vessels simultaneously, we applied a logical OR operation to the results, resulting in the Figure 3

The combined image showcases the detection of both thin and thick vessels.

### Hyperparameter Experimental Results

Different hyperparameter experiments and their output are summarized in the Table 2

Experiment	s	L	c	W
1	0.5	2	2.3	31
2	0.5	2	5	31
3	1	5	2.3	2
4	1	5	2.3	90
5	2	9	0.5	31
6	2	12	0.5	31
7	3	9	5	31
8	3	12	5	31

Table 2: Hyperparameter Experiments

The corresponding figures for each experiment are shown in Figure 4.

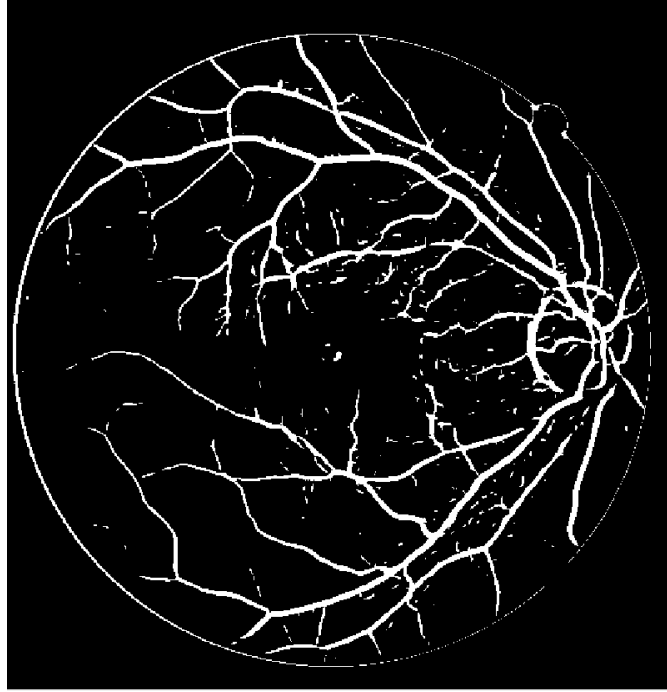


Figure 3: Combined Vessels Detection Result

## Comparison of Experiments

### Effect of Hyperparameter Variations on Retinal Vessel Detection

In the implementation of retinal vessel extraction by a matched filter with first-order derivative of Gaussian, various hyperparameters were systematically varied to observe their influence on the edge detection of blood vessels in pathological retinal images. The following is a comparative analysis of the outcomes resulting from these variations.

#### Scale ( $s$ )

The scale parameter influences the detection sensitivity relative to the size of the blood vessels. Smaller scales, such as  $s = 0.5$ , enhance the filter's capability to detect finer vessels, albeit at the risk of introducing more noise. Conversely, larger scales like  $s = 3$  may overlook finer details but offer a clearer view of prominent vessels.

#### Length ( $L$ )

The length parameter dictates the degree of noise smoothing along the Y-axis. An optimal value is critical; too low may lead to insufficient noise reduction, while too high can erase critical vessel details. For instance,  $L = 2$  appears to strike a balance between edge preservation and noise mitigation.



**Constant ( $c$ )**

This empirical constant is pivotal for calculating the threshold for vessel detection. Lower constants ( $c = 0.5$ ) tend to include more pixels as part of vessels, which may not always correspond to true vessel edges, indicating a lower specificity. A higher constant ( $c = 2.3$ ) yields a more conservative detection, potentially increasing specificity but decreasing sensitivity.

**Window Size ( $W$ )**

Window size impacts local averaging and thus the smoothness of the resultant image. Smaller windows ( $W = 2$ ) retain detailed features at the expense of noise reduction. Larger windows ( $W = 90$ ), while reducing noise significantly, might cause a loss of important vessel edge information.

Each parameter needs to be adjusted to achieve an optimal balance between detailed vessel edge detection and noise reduction. The choice of parameters is heavily dependent on the characteristics of the input image.

**Visual and Quantitative Analysis** Visually, lower scales and constants are preferable for detailed images with minimal noise, whereas higher values are better suited for noisier images or when focusing on larger vessels. The length and window size selection should be tailored to the detail requirement and noise level of the images. A comparative analysis is enriched by including quantitative metrics like sensitivity and specificity, providing a more comprehensive understanding of the hyperparameters' impact on the vessel extraction algorithm's performance.

**Reflection on the Implementation Process****• Pros of the Implemented Method:**

- *Sensitivity to Vessel Size:* The use of scale as a parameter allows for the detection of blood vessels of varying sizes, which can be particularly beneficial for detailed analysis of retinal images.
- *Noise Reduction:* By adjusting the length and window size parameters, the method effectively reduces noise, thereby enhancing the clarity of vessel detection.
- *Empirical Optimization:* The constant  $c$  provides a means to fine-tune the algorithm based on empirical experience, thus tailoring the detection threshold to specific datasets.

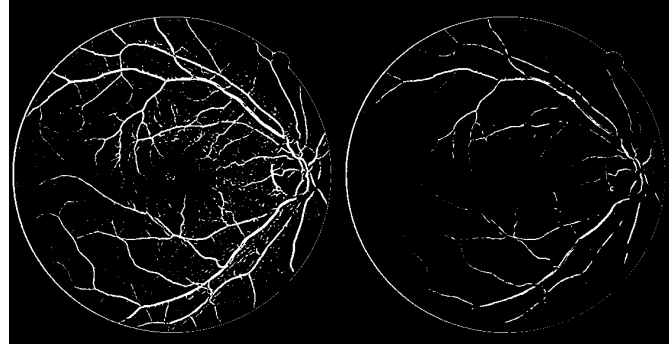
**• Cons of the Implemented Method:**

- *Complex Parameter Tuning:* The need to adjust multiple hyperparameters can make optimization complex and time-consuming.

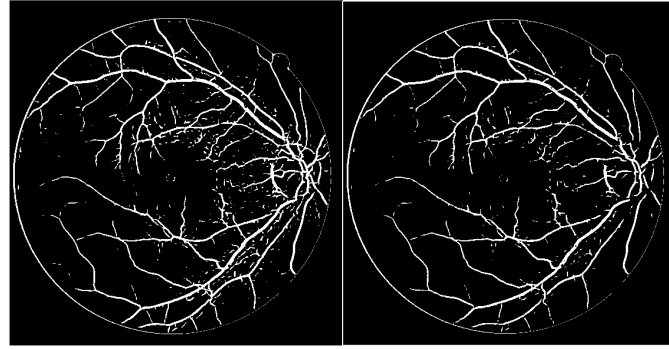
- *Trade-Off Between Detection and Noise:* Achieving a balance between sensitivity to small vessels and noise reduction often requires a compromise that may not be ideal for all cases.
- *Dependence on Image Quality:* The effectiveness of the method is highly dependent on the quality of the input image, with poor quality images posing significant challenges to vessel detection.

- **Difficulties in Reimplementation:**

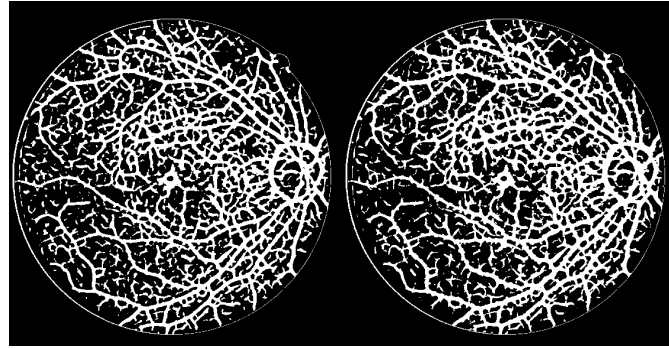
- *Parameter Calibration:* Determining the optimal set of hyperparameters was challenging due to the variability in retinal image characteristics.
- *Algorithm Complexity:* The multifaceted nature of the algorithm, involving several preprocessing and postprocessing steps, required a steep learning curve for the team.



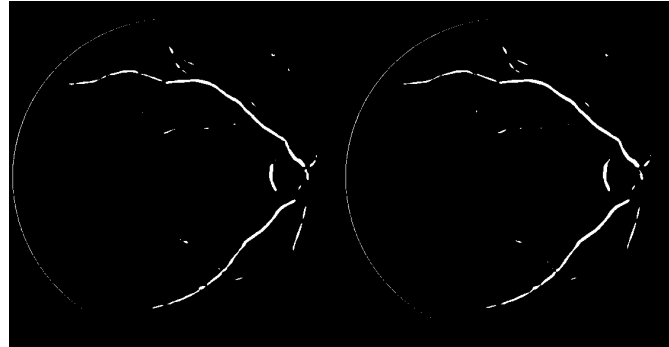
(a)  $s=0.5$ ,  $L=2$ ,  $c=2.3$ ,  $W=31$     (b)  $s=0.5$ ,  $L=2$ ,  $c=5$ ,  $W=31$



(c)  $s=1$ ,  $L=5$ ,  $c=2.3$ ,  $W=2$     (d)  $s=1$ ,  $L=5$ ,  $c=2.3$ ,  $W=90$



(e)  $s=2$ ,  $L=9$ ,  $c=0.5$ ,  $W=31$     (f)  $s=2$ ,  $L=12$ ,  $c=0.5$ ,  $W=31$



(g)  $s=3$ ,  $L=9$ ,  $c=5$ ,  $W=31$     (h)  $s=3$ ,  $L=12$ ,  $c=5$ ,  $W=31$

Figure 4: Experimental Results for Different Hyperparameters

## References

- [1] S. Chaudhuri et al. “Detection of Blood Vessels in Retinal Images Using Two-Dimensional Matched Filters”. In: *IEEE Trans. Med. Imaging* 8.3 (1989), pp. 263–269.
- [2] Jyotiprava Dash, Priyadarsan Parida, and Nilamani Bhoi. “Retinal Blood Vessel Extraction from Fundus Images Using Enhancement Filtering and Clustering”. In: *Electronic Letters on Computer Vision and Image Analysis* 19 (July 2020), pp. 38–52. DOI: 10.5565/rev/elcvia.1239.
- [3] A. Hoover, V. Kouznetsova, and M. Goldbaum. “Locating Blood Vessels in Retinal Images by Piecewise Threshold Probing of a Matched Filter Response”. In: *IEEE Trans. Med. Imaging* 19.3 (2000), pp. 203–210.
- [4] Bob Zhang et al. “Retinal Vessel Extraction by Matched Filter with First-Order Derivative of Gaussian”. In: *Computers in Biology and Medicine* (2010), pp. 438–445.